

Transport of active ellipsoidal particles in ratchet potentials

Bao-quan Ai* and Jian-chun Wu

*Laboratory of Quantum Engineering and Quantum Materials,
School of Physics and Telecommunication Engineering,
South China Normal University, 510006 Guangzhou, China.*

(Dated: May 12, 2015)

Rectified transport of active ellipsoidal particles is numerically investigated in a two-dimensional asymmetric potential. The out-of-equilibrium condition for the active particle is an intrinsic property, which can break thermodynamical equilibrium and induce the directed transport. It is found that the perfect sphere particle can facilitate the rectification, while the needlelike particle destroys the directed transport. There exist optimized values of the parameters (the self-propelled velocity, the torque acting on the body) at which the average velocity takes its maximal value. For the ellipsoidal particle with not large asymmetric parameter, the average velocity decreases with increasing the rotational diffusion rate, while for the needlelike particle (very large asymmetric parameter), the average velocity is a peaked function of the rotational diffusion rate. By introducing a finite load, particles with different shapes (or different self-propelled velocities) will move to the opposite directions, which is able to separate particles of different shapes (or different self-propelled velocities).

PACS numbers: 05. 60. Cd, 05. 40. -a, 82. 70. Dd

Keywords: self-propelled particles, ellipsoidal particles, Brownian ratchet

I. INTRODUCTION

Noise-induced transport far from equilibrium plays a crucial role in many processes from physical and biological to social systems. The transport properties of systems consisting of active particles have generated much attention. There are numerous realizations of active particles^{1,2} in nature ranging from bacteria³⁻⁶ and spermatozoa⁷ to artificial colloidal microswimmers. Self-propulsion is an essential feature of most living systems, which can maintain metabolism and perform movement. The kinetic of self-propulsion particles moving in potentials could exhibit peculiar behavior⁸⁻²². The problem of rectifying motion in random environments is an important issue, which has many theoretical and practical implications²³. At equilibrium the periodic potential alone is not able to produce a rectification effect, due to the detailed balance preventing time symmetry breaking. Indeed, one has to add some perturbation which breaks the time symmetry and brings the system out of equilibrium. For the active particles, the out-of-equilibrium condition is an intrinsic property of the system. So the active particle without any external forces can break the symmetry of the system and be rectified in periodic systems.

Recently, rectification of self-propelled particles in asymmetric external potentials has attracted much attention. Angelani and co-workers²⁴ studied the run-and-tumble particles in periodic potentials and found that the asymmetric potential produces a net drift speed. Even in the symmetric potential a spatially modulated self-propulsion and a phase shift against the potential can induce the directed transport²⁵. Recently, transport of Janus particles in periodically compartmentalized channel is investigated²⁶ and the rectification can be orders

of magnitude stronger than that for ordinary thermal potential ratchets. In all these studies²⁴⁻²⁶ on active ratchet, the active particle was treated as the point spherical particle.

However, shape deformation of particles plays an important role in nonequilibrium transport processes²⁷⁻³². Han and co-workers²⁷ experimentally studied the Brownian motion of isolated ellipsoid particles in two dimensions and quantified the crossover from short-time anisotropic to long-time isotropic diffusion. In the presence of an external potential, the external force can amplify the non-Gaussian character of the spatial probability distributions²⁸. Ohta and co-workers²⁹ found that an isolated deformable particle exhibits a bifurcation such that a straight motion becomes unstable and a circular motion appears. Due to the coupling of the rotational and translational motion, Brownian motion of asymmetrical particles is considerably more complicated compared to the spherical case, and thus shows peculiar behavior. Therefore, how active asymmetrical particles are rectified from a ratchet potential may receive much attention. In this paper, we will extend the study of active ratchet from the spherical particle to the asymmetric particle. We focus on finding how the asymmetry of the particle affects the rectified transport and how asymmetric particles can be separated.

II. MODEL AND METHODS

We consider an ellipsoidal (anisotropic) particle moving in a two-dimensional ratchet potential (shown in Fig. 1). The particle is self-propelled along its long axis. In the lab x - y frame, the particle at a given time t can be described by the position vector $\vec{R}(t)$ of its center of mass,

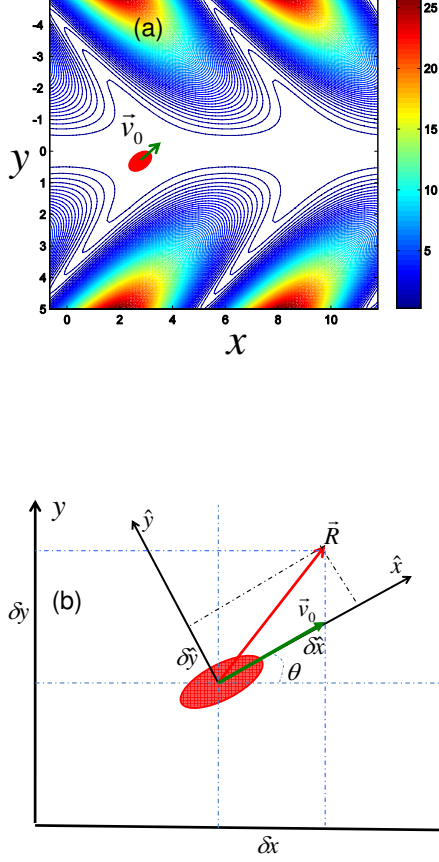


FIG. 1: Schematic diagram illustrating the system. (a) The active particle with the self-propelled velocity moving in the ratchet potential and the equipotentials of the potential described by Eq.(13). (b) Representation of an ellipsoid in the x - y lab frame and the \hat{x} - \hat{y} body frame. The angle between two frames is θ . The displacement \vec{R} can be decomposed as $(\delta\hat{x}, \delta\hat{y})$ or $(\delta x, \delta y)$.

which also corresponds to the coordinates in the body frame $(\delta\hat{x}, \delta\hat{y})$. $\theta(t)$ is the angle between the x axis of the lab frame and the \hat{x} axis of the body frame. Rotational and translational motion in the body frame are always decoupled, so the dynamics of the active ellipsoid particle is described by the Langevin equations in this frame^{27,28},

$$\frac{1}{\Gamma_1} \frac{\partial \hat{x}}{\partial t} = F_x \cos \theta(t) + F_y \sin \theta(t) + \hat{\xi}_1(t) + \frac{v_0}{\Gamma_1} \quad (1)$$

$$\frac{1}{\Gamma_2} \frac{\partial \hat{y}}{\partial t} = F_y \cos \theta(t) - F_x \sin \theta(t) + \hat{\xi}_2(t), \quad (2)$$

$$\frac{1}{\Gamma_3} \frac{\partial \theta(t)}{\partial t} = \tau + \hat{\xi}_3(t), \quad (3)$$

where v_0 is the self-propelled velocity in the body frame, which is taken along the long axis of the ellipsoid particle. Γ_1 and Γ_2 are the mobilities along its long and short axis, respectively. Γ_3 is the rotational mobility and τ is the torque acting on the body due to its orientation relative to the direction of the potential. F_x and F_y are the forces along x and y direction of the lab frame. The noise $\hat{\xi}_i(t)$ has mean zero and satisfies

$$\langle \hat{\xi}_i(t) \hat{\xi}_j(t') \rangle = \frac{2k_B T}{\Gamma_i} \delta_{i,j} \delta(t - t'), i, j = 1, 2, 3, \quad (4)$$

where T is the temperature and k_B is the Boltzmann constant.

We now obtain these equations in the lab frame based on the method described in Ref.²⁸. By means of a straight forward rotation of coordinates, the displacement in the two frames are related by the following equations,

$$\delta x = \cos \theta \delta \hat{x} - \sin \theta \delta \hat{y}, \quad (5)$$

$$\delta y = \sin \theta \delta \hat{x} + \cos \theta \delta \hat{y}. \quad (6)$$

After somewhat manipulations, Eqs. (1,2,3) in the body frame can be replaced by the following equations in the lab frame^{27,28}

$$\frac{\partial x}{\partial t} = v_0 \cos \theta(t) + F_x \left[\bar{\Gamma} + \Delta \Gamma \cos 2\theta(t) \right] + \Delta \Gamma F_y \sin 2\theta(t) + \xi_1(t), \quad (7)$$

$$\frac{\partial y}{\partial t} = v_0 \sin \theta(t) + F_y \left[\bar{\Gamma} - \Delta \Gamma \cos 2\theta(t) \right] + \Delta \Gamma F_x \sin 2\theta(t) + \xi_2(t), \quad (8)$$

$$\frac{\partial \theta(t)}{\partial t} = \Gamma_3 \tau + \xi_3(t), \quad (9)$$

where the quantities $\bar{\Gamma} = \frac{1}{2}(\Gamma_1 + \Gamma_2)$ and $\Delta \Gamma = \frac{1}{2}(\Gamma_1 - \Gamma_2)$ are the average and difference mobilities of the body, respectively. The parameter $\Delta \Gamma$ determines the asymmetry of the body, the particle is a perfect sphere for $\Delta \Gamma = 0$ and a very needlelike ellipsoid for $\Delta \Gamma \rightarrow \bar{\Gamma}$. The noise $\xi_i(t)$ has mean zero and the following relations^{27,28}

$$\langle \xi_3(t) \xi_3(t') \rangle = 2D_\theta \delta(t - t'), \quad (10)$$

$$\langle \xi_i(t) \xi_j(t') \rangle_{\theta(t)}^{\xi_1, \xi_2} = 2k_B T \Gamma_{ij} \delta(t - t'), \quad (11)$$

and

$$\Gamma_{ij} = \bar{\Gamma} \delta_{ij} + \Delta \Gamma \begin{pmatrix} \cos 2\theta & \sin 2\theta \\ \sin 2\theta & -\cos 2\theta \end{pmatrix}, \quad (12)$$

where $D_\theta = k_B T \Gamma_3$ is the rotational diffusion rate, which describes the nonequilibrium angular fluctuation. The

statistical averages have superscripts to indicate over which noise is the average taken and subscripts to denote quantities which are kept fixed.

For the asymmetric potential, we consider the following potential³³ (shown in Fig. 1(a)),

$$U(x, y) = \frac{U_0}{2} y^2 [\cos(x + \Delta \ln \cosh y) + 1.1] + fx, \quad (13)$$

where U_0 is the height of the potential and f is the load along the x direction. Δ is the asymmetric parameter of the potential and the potential is symmetric at $\Delta = 0.0$. The equipotentials are now symmetry broken and look like a herringbone pattern for $\Delta \neq 0$.

In this paper, we focus on the direction transport of active asymmetrical particles. The behavior of the quantities of interest can be corroborated by Brownian dynamic simulations performed by integration of the Langevin equations (7,8,9) using the second-order stochastic Runge-Kutta algorithm. Because the particle along the y -direction is confined, we only calculate the x -direction average velocity based on Eqs. (7,8,9),

$$v_{\theta_0} = \lim_{t \rightarrow \infty} \frac{\langle x(t) \rangle_{\theta_0}^{\xi_1, \xi_2}}{t}, \quad (14)$$

where θ_0 is initial angle of the trajectory. The full average velocity after a second average over all θ_0 is

$$v = \frac{1}{2\pi} \int_0^{2\pi} d\theta_0 v_{\theta_0}. \quad (15)$$

For the convenience of discussion, we define the scaled average velocity $v_s = v/v_0$ through the paper. In our simulations, the integration step time Δt was chosen to be smaller than 10^{-4} and the total integration time was more than 3×10^5 and the transient effects were estimated and subtracted. The stochastic averages reported above were obtained as ensemble averages over 3×10^4 trajectories with random initial conditions.

III. RESULTS AND DISCUSSION

Based on the numerical simulations, we mainly calculate the average velocity for the two cases: zero load and finite load. For the zero load case, we focus on the rectification effects and how the parameters can affect rectification. For the finite load case, we present two particle separation methods: shape separation and self-propelled velocity separation. In the simulations, unless otherwise noted, we set $k_B T = 1.0$, $\tau = 0.0$, $\bar{\Gamma} = 1.0$, and $U_0 = 1.0$ throughout the paper.

A. Zero load and rectification

We first consider the zero load case ($f = 0.0$). The scaled average velocity v_s as a function of asymmetrical

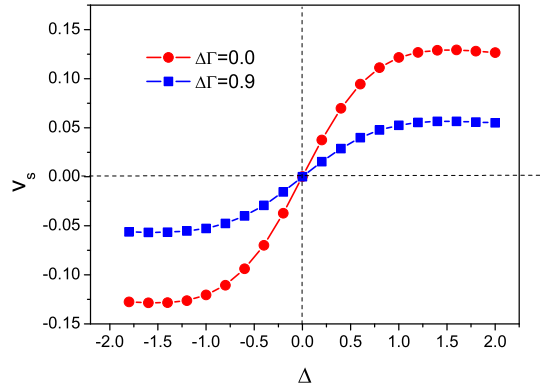


FIG. 2: Scaled average velocity v_s as a function of the asymmetrical parameter Δ of the potential for different values of $\Delta\Gamma$ at $v_0 = 2.0$ and $D_\theta = 0.1$.

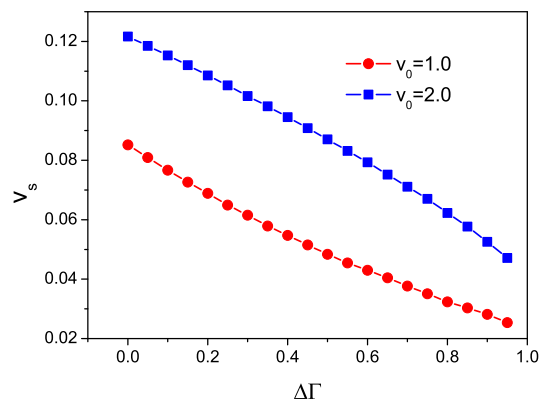


FIG. 3: Scaled average velocity v_s as a function of the asymmetrical parameter $\Delta\Gamma$ of the particle for different values of v_0 at $\Delta = 1.0$, $f = 0.0$, and $D_\theta = 0.1$.

parameter Δ of the potential is reported in Fig. 2. It is found that v_s is positive for $\Delta > 0$, zero at $\Delta = 0$, and negative for $\Delta < 0$. A qualitative explanation of this behavior can be given by the following argument. For $\Delta = 0$ (symmetric case) the probabilities of crossing right and left barriers are the same and then there is a null net particles flow. For $\Delta > 0$, the left side from the minima of the potential is steeper, it is easier for particles to move toward the gentler slope side than toward the steeper side, so the average velocity is positive. Therefore, the asymmetry of the potential will determine the direction of the transport and no directed transport occurs in a symmetric potential.

The dependence of the scaled average velocity v_s on the asymmetrical parameter $\Delta\Gamma$ of the particle is presented in Fig. 3 at $\Delta = 1.0$. We find that v_s decreases monotonically with the increase of the asymmetrical parameter $\Delta\Gamma$. In order to give the explanation of the

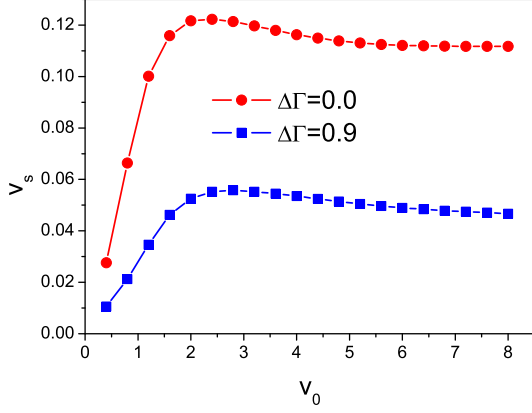


FIG. 4: Scaled average velocity v_s as a function of the self-propelled velocity v_0 for different values of $\Delta\Gamma$ at $\Delta = 1.0, f = 0.0$, and $D_\theta = 0.1$.

phenomenon, we present the translational diffusion coefficient in the x direction²⁸ $D_{xx} = D_0 + \frac{\Delta\Gamma^2(F_x^2 + F_y^2)}{8D_\theta}$, where $D_0 = k_B T \bar{\Gamma}$. As we know, the increase of D_{xx} enhances the ratchet effect when $D_{xx} < U_0$ and reduces the ratchet effect when $D_{xx} > U_0$. When $D_{xx} \simeq U_0$, the optimized ratchet effect occurs. In our system, $D_0 = 1.0$ and $U_0 = 1.0$, the ratchet effect is optimized when $\Delta\Gamma = 0$ ($D_{xx} = U_0$). As $\Delta\Gamma$ increases from zero, $D_{xx} > U_0$, the ratchet effect is gradually destroyed and v_s decreases monotonically. Therefore, the perfect sphere particle can facilitate the rectification, while the needlelike ellipsoid particle destroys the directed transport.

From Fig. 3, we can also find that the curve is convex for large value v_0 and concave for small value v_0 . This phenomenon can be easily explained by introducing the two factors: (A) the increase of v_0 (from 0 to 2) enhances the transport (shown in Fig. 4) and (B) the increase of $\Delta\Gamma$ reduces the transport. For small value v_0 ($v_0 = 1.0$), on increasing $\Delta\Gamma$, factor B firstly dominates the transport, v_s reduces quickly, and finally the ratchet effect gradually disappears (very small value v_s), v_s reduces slowly, so the curve is concave. For $v_0 = 2.0$, on increasing $\Delta\Gamma$, factor A firstly determines the transport, v_s reduces slowly, and finally factor B also becomes important, v_s reduces quickly, so the curve is convex.

Figure 4 shows the scaled average velocity v_s as a function of the self-propelled velocity v_0 . The term $v_0 \cos \theta(t)$ in Eq. (7) can be seen as the external driving force. When $v_0 \rightarrow 0$, the external driving force can be negligible, so the average velocity will tend to zero. For very large values of v_0 , the effect of the asymmetry of the potential reduces, thus v_s becomes small. Therefore, there exists an optimal value of v_0 at which v_s takes its maximal value. So the optimal self-propelled velocity can facilitate the rectification of particles.

Results for v_s as a function of the rotational diffu-

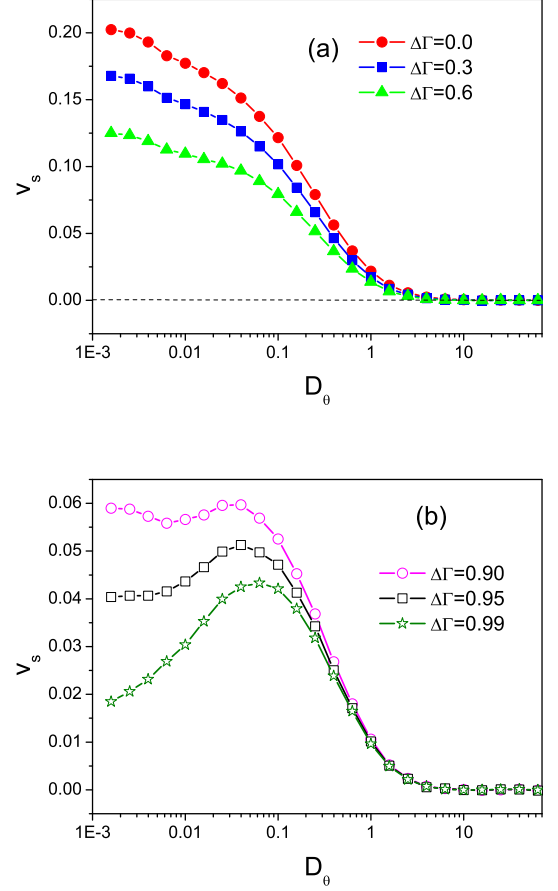


FIG. 5: Scaled average velocity v_s as a function of the rotational diffusion rate D_θ for different values of $\Delta\Gamma$. (a) ellipsoidal particles ($\Delta\Gamma = 0, 0.3, 0.6$). (b) needlelike particles ($\Delta\Gamma = 0.9, 0.95, 0.99$). The other parameters are $\Delta = 1.0$, $f = 0.0$, and $v_0 = 2.0$.

sion rate D_θ are presented in Fig. 5 for different values of $\Delta\Gamma$. For the case of ellipsoidal particles ($\Delta\Gamma = 0, 0.3, 0.6$) shown in Fig. 5(a), the scaled average velocity v_s decreases with the increase of D_θ . The term $v_0 \cos \theta(t) (\propto v_0 \cos(D_\theta t))$ in Eq. (7) can be seen as the external driving force along x -direction. In the adiabatic limit $D_\theta \rightarrow 0$, the external force can be expressed by two opposite static forces v_0 and $-v_0$, yielding the mean velocity $V = \frac{1}{2}[v(v_0) + v(-v_0)]$, which is similar to the adiabatic case in the forced thermal ratchet²³. As D_θ increases, the scaled average velocity v_s decreases. When $D_\theta \rightarrow \infty$, the self-propelled angle changes very fast, particles are trapped in the valley of the potential, so v_s tends to zero, which is similar to the high frequency driving case in the forced thermal ratchet³⁴.

However, for the case of needlelike particles ($\Delta\Gamma = 0.9, 0.95, 0.99$) shown in Fig 5 (b), the anisotropic diffusion dominates the transport and there exists an optimal value of $\Delta\Gamma$ at which v_s takes its maximal value. This

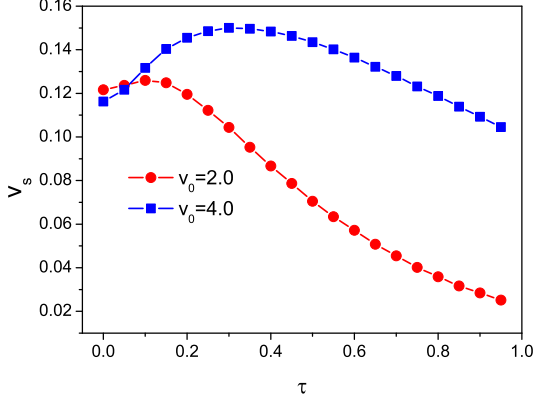


FIG. 6: Scaled average velocity v_s as a function of the torque τ acting on the body for different values of v_0 at $\Delta = 1.0, f = 0.0, D_\theta = 0.1$, and $\Delta\Gamma = 0.0$.

is due to the mutual interplay between the anisotropic diffusion and the rotational diffusion rate. There are two time periods in the system: the anisotropic diffusion time $\tau_D = \frac{4\pi^2}{D_{xx}}$ for crossing one period of the potential along x -direction and the period $\tau_\theta = \frac{2}{D_\theta}$ for direction randomly varying in time. For the case of needlelike particles, the anisotropic diffusion time becomes very important. When these two time periods cooperate with each other, the optimized rectification will occur.

Figure 6 describes the dependence of the scaled average velocity v_s on the torque τ for different values of v_0 . From Eq. (9), we can see that the self-propelled angle $\theta(t)$ is determined by the torque and the random noise. When $\tau \rightarrow 0$, the rotational diffusion rate determines the angle $\theta(t)$. On increasing τ , both the torque and the random noise play the important roles and work together in the transport, which induces the maximal average velocity. However, when $\tau \rightarrow \infty$, the self-propelled angle changes very fast, particles are trapped in the valley of the potential and v_s goes to zero. Therefore, large torque would suppress strongly the ratchet effect.

B. Finite load and particle separation

Since transport behaviors in the present system strongly depend on the asymmetric parameter $\Delta\Gamma$ of the particle and the self-propelled velocity v_0 , it is possible to realize particle separation. We will present two particle separation mechanisms which induce the motion of particles of different $\Delta\Gamma$ or v_0 in opposite directions by introducing an external load f on the x -direction.

Figure 7 (a) shows the scaled average velocity as a function of the load f for different values of $\Delta\Gamma$. For small values of f , the positive ratchet effect dominates the transport and the average velocity is positive. On increasing the load f , the load dominates the transport,

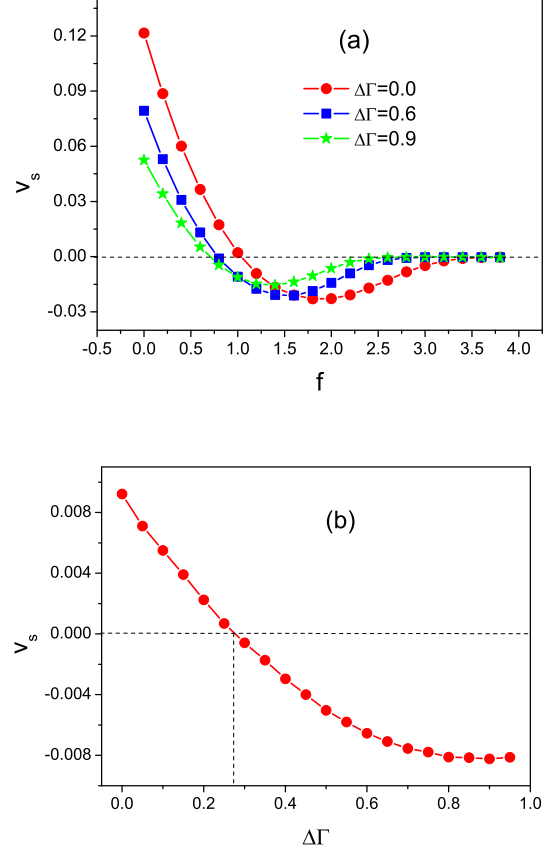


FIG. 7: (a) Scaled average velocity v_s as a function of the load f for different values of $\Delta\Gamma$. (b) Scaled average velocity v_s as a function of the parameter $\Delta\Gamma$ at $f = 0.9$. The other parameters are $\Delta = 1.0$ and $v_0 = 2.0$, and $D_\theta = 0.1$.

the average velocity crosses zero and subsequently reverses its direction. For very large load, particles are blocked and v_s tends to zero exponentially. From Fig. 1(a), we can find that if the load f is negative (positive force along x -direction), the particle will move forward without problem. If the load f is positive (negative force along x -direction), the particle will move backward and may get into a spine of the herringbone. Thus, the particle has to go against the force in order to climb back up and get again on the backbone. Moreover, one can find that the stronger the force, the deeper the spine. Therefore, the particle is blocked in the spines for very large values of f . Note that this blocked phenomenon had been explained detailedly in Ref.³³. There exists a valley in the curve $v_s - f$ at which the average velocity takes its negative maximal value. The position of the valley varies with $\Delta\Gamma$. For a given load ($f = 0.9$) shown in Fig. 7 (b), the asymmetric parameter $\Delta\Gamma$ of the particle can determine the direction of the transport. Particles larger than the threshold asymmetric parameter $\Delta\Gamma_c$ move to the left, whereas particles smaller than that move to the

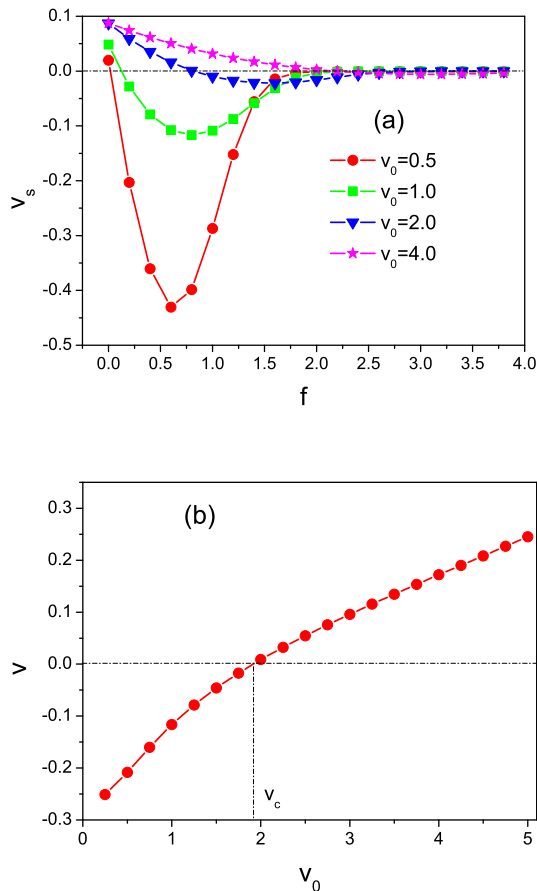


FIG. 8: (a) Scaled average velocity v_s as a function of the load f for different values of v_0 . (b) Average velocity v as a function of v_0 at $f = 0.75$. The other parameters are $\Delta = 1.0$ and $\Delta\Gamma = 0.5$, and $D_\theta = 0.1$.

right. Therefore, one can separate particles of different values of $\Delta\Gamma$ and make them move in opposite directions.

Figure 8 (a) shows the scaled average velocity as a function of the load f for different values of the self-propelled velocity v_0 . There exist two driving factors in the system: (1) the self-propelled velocity v_0 which induces the positive current; (2) the load f which causes the negative current. For small values of v_0 (e. g. $v_0 = 0.5$), the load f dominates the transport and the self-propelled velocity v_0 can be neglected. When $f \rightarrow 0$, the average velocity goes to zero. When increasing f , the amplitude of the negative velocity increases. However, for very large values of f , the particle is blocked and the average velocity tends to zero. Therefore, there exists a valley in the curve $v_s - f$ at which the average velocity takes its negative maximal value. However, on increasing v_0 , the self-propelled velocity driving factor becomes more important and the positive current gradually dominates the average velocity. Therefore, the valley in the curve grad-

ually disappears. Therefore, the self-propelled velocity v_0 strongly affects the transport and even determines its direction. For a given value of f (e. g. 0.75) shown in Fig. 8 (b), particles with larger than the threshold velocity v_c move to the right, whereas particles smaller than that move to the left. Therefore, one can separate particles of different values of v_0 and make them move in opposite directions.

Note that there are some other methods which can separate particles for our system. Particles can be separated if their drift speeds are different, no need to move in the opposite directions. Particles with different shapes can be separated by many other means rather than the ratchet method. However, our separation methods (which make particles move in opposite directions) are more effective and feasible.

IV. CONCLUDING REMARKS

In this work we have studied the transport of active ellipsoidal particles in a two-dimensional asymmetric potential by numerical simulations. It is found that the self-propelled velocity can break thermodynamical equilibrium and induce directed transport. The direction of the transport is determined by the asymmetry of the potential. The shape of particles can strongly affect the rectified transport, the perfect sphere particle can facilitate the rectification, while the needlelike particle destroys the directed transport. There exist optimized values of the parameters (the self-propelled velocity, the torque acting on the body) at which the average velocity takes its maximal value. For the ellipsoidal particle with not large asymmetric parameter, the average velocity decreases with increasing the rotational diffusion rate, while for the needlelike particle (very large $\Delta\Gamma$), the average velocity is a peaked function of the rotational diffusion rate. In addition, by introducing a finite load on particles, we have presented two particle separation ways (1) shape separation: particles larger than the critical asymmetric parameter $\Delta\Gamma_c$ move to the left, whereas particles smaller than that move to the right; (2) self-propelled velocity separation: particles with larger than the threshold velocity v_c move to the right, whereas particles smaller than that move to the left. Therefore, one can separate particles of different shapes (or different self-propelled velocities) and make them move in opposite directions. The results we have presented have a wide application in many systems, such as spontaneously moving oil droplets, motor proteins, bacterial swimmers, and motile cells.

This work was supported in part by the National Natural Science Foundation of China (Grant No. 11175067), the PCSIRT (Grant No. IRT1243), the Natural Science Foundation of Guangdong Province, China (Grant No. S2011010003323), the Scientific Research Foundation of Graduate School of South China Normal University.

-
- * Email: aibq@scnu.edu.cn
- ¹ E. Lauga and T. R. Powers, Rep. Prog. Phys. 72, 096601 (2009).
 - ² J. Toner, Y. Tu, and S. Ramaswamy, Annals of Physics 318, 170 (2005).
 - ³ K. C. Leptos, J. S. Guasto, J. P. Gollub, A. I. Pesci, and R. E. Goldstein, Phys. Rev. Lett., 103, 198103 (2009).
 - ⁴ R. Di Leonardo, L. Angelani, D. DellArciprete, G. Ruocco, V. Iebba, S. Schippa, M. P. Conte, F. Mecarini, F. De Angelis, and E. Di Fabrizio, Proc. Natl. Acad. Sci. USA 107, 9541 (2010); V. B. Shenoy, D. T. Tambe, A. Prasad, and J. A. Theriot, Proc. Natl. Acad. Sci. USA 104, 8229 (2007).
 - ⁵ J. Hill, O. Kalkanci, J. L. McMurtry, and H. Koser, Phys. Rev. Lett. 98, 068101 (2007).
 - ⁶ W. R. DiLuzio, L. Turner, M. Mayer, P. Garstecki, D. B. Weibel, H. C. Berg, and G. M. Whitesides, Nature 435, 1271 (2005).
 - ⁷ I. H. Riedel, K. Kruse, and J. Howard, Science, 309, 300(2005).
 - ⁸ P. S. Burada and B. Lindner, Phys. Rev. E 85, 032102 (2012).
 - ⁹ F. Schweitzer, W. Ebeling, and B. Tilch, Phys. Rev. Lett. 80, 5044 (1998).
 - ¹⁰ J. Tailleur and M. E. Cates, Phys. Rev. Lett. 100, 218103 (2008).
 - ¹¹ R. Großmann, L. Schimansky-Geier, and P. Romanczuk, New J. Phys. 14, 073033 (2012).
 - ¹² A. Kaiser, K. Popowa, H. H. Wensink, and H. Löwen, Phys. Rev. E 88, 022311 (2013).
 - ¹³ Y. Fily and M. C. Marchetti, Phys. Rev. Lett. 108, 235702 (2012); S. Henkes, Y. Fily, and M. C. Marchetti, Phys. Rev. E 84, 040301 (2011).
 - ¹⁴ F. Kummel, B. ten Hagen, R. Wittkowski, I. Buttinoni, R. Eichhorn, G. Volpe, H. Löwen, and C. Bechinger, Phys. Rev. Lett. 110, 198302 (2013); I. Buttinoni, J. Bialke, F. Kummel, H. Löwen, C. Bechinger, and T. Speck, Phys. Rev. Lett. 110, 238301 (2013).
 - ¹⁵ T. Bickel, A. Majee, and A. Wurger, Phys. Rev. E 88, 012301 (2013).
 - ¹⁶ S. Mishra, K. Tunstrom, I. D. Couzin, and C. Huepe, Phys. Rev. E 86, 011901 (2012).
 - ¹⁷ A. Czirák, A. L. Barabási, and T. Vicsek, Phys. Rev. Lett. 82, 209 (1999).
 - ¹⁸ F. Peruani, T. Klaus, A. Deutsch, and A. Voss-Boehme, Phys. Rev. Lett. 106, 128101 (2011).
 - ¹⁹ C. Weber, P. K. Radtke, L. Schimansky-Geier, and P. Hänggi, Phys. Rev. E 84, 011132 (2011).
 - ²⁰ M. Enculescu and H. Stark, Phys. Rev. Lett. 107, 058301 (2011).
 - ²¹ B. Q. Ai, Q. Y. Chen, Y. F. He, W. R. Zhong, in prepration.
 - ²² H. Chen and Z. Hou, Phys. Rev. E 86, 041122 (2012)
 - ²³ P. Reimann, Phys. Rep. 361, 57 (2002); P. Hänggi and F. Marchesoni, Rev. Mod. Phys. 81, 387 (2009).
 - ²⁴ L. Angelani, A. Costanzo, and R. Di Leonardo, EPL, 96, 68002 (2011).
 - ²⁵ A. Pototsky, A. M. Hahn, and H. Stark, Phys. Rev. E 87, 042124 (2013).
 - ²⁶ P. K. Ghosh, V. R. Misko, F. Marchesoni, and F. Nori, Phys. Rev. Lett. 110, 268301 (2013).
 - ²⁷ Y. Han, A. M. Alsayed, M. Nobili, J. Zhang, T. C. Lubensky, A. G. Yodh, Science 314, 626 (2006); Y. Han, A. Alsayed, M. Nobili, and A. G. Yodh, Phys. Rev. E 80, 011403 (2009).
 - ²⁸ R. Grima and S. N. Yaliraki, J. Chem. Phys. 127, 084511 (2007); R. Grima, S. N. Yaliraki, and M. Barahona, J. Phys. Chem. B 114, 5380 (2010).
 - ²⁹ T. Ohta and T. Ohkuma, Phys. Rev. Lett. 102, 154101 (2009); M. Tarama and T. Ohta, Phys. Rev. E 87, 062912 (2013).
 - ³⁰ M. Y. Matsuo, H. Tanimoto, and M. Sano, EPL 102, 40012 (2013).
 - ³¹ G. Mammadov, arXiv:1205.0294.
 - ³² I. Gralinski, A. Neild, T. W. Ng, and M. S. Muradoglu, J. Chem. Phys. 134, 064514 (2011).
 - ³³ G. A. Cecchi and M. O. Magnasco, Phys. Rev. Lett. 76, 1968 (1996).
 - ³⁴ B. Q. Ai, Phys. Rev. E 80, 011113 (2009); D. Dan, M. C. Mahato, and A. M. Jayannavar, Phys. Rev. E 63, 056307 (2001).